PROCEEDINGS OF SCIENCE

High-Efficiency WLS Plastic: Enhancing Compact Cherenkov-Based Velocity Measurements

F. Nozzoli,[a,*] L.E. Ghezzer,[b] F. Bruni,[c,d] F. Meinardi,[c,d] R. Nicolaidis,[b] L. Ricci,[b] E. Verroi,[a] P. Spinnato[a] and P. Zuccon[b]

[a] *INFN Trento Institute for Fundamental Physics and Applications, Via Sommarive 14, 38123 Trento, Italy*
[b] *Physics Department, Trento University, Via Sommarive 14, 38123 Trento, Italy*
[c] *Dipartimento Scienza dei Materiali, Università di Milano Bicocca, Milano Italy*
[d] *Glass to Power s.p.a., Via Fortunato Zeni 8 - Rovereto - Italy*

E-mail: francesco.nozzoli@unitn.it

Cherenkov radiation, produced when a charged particle propagates faster than the phase velocity of light within a dielectric medium, represents a well-established tool for particle identification. The number of Cherenkov visible photons is nevertheless modest, usually on the order of 100-200 per centimeter of track length in common media such as glass, water, or plastic. In the present work we examine the optical behavior of FB118, a Wavelength Shifting (WLS) plastic manufactured by Glass to Power, when it is exposed to ionizing particles. Our observations clearly show that FB118 exhibits no residual scintillation, thus permitting an unambiguous identification of Cherenkov emission. Furthermore, thanks to its intrinsic WLS characteristics, the material increases of a factor $\times 10$ the collection of photons in the visible spectrum. Taken together, these properties suggest that FB118 is a strong candidate for compact Cherenkov detector designs, especially in astroparticle physics applications where limitations in space and power call for efficient and miniaturized solutions.

39th International Cosmic Ray Conference (ICRC2025)
15–24 July 2025
Geneva, Switzerland

*Speaker

PoS(ICRC2025)103

1. Introduction

When a charged particle moves through a dielectric material with a velocity greater than the speed of light in that medium, it gives rise to the Cherenkov effect. This process results in the emission of coherent electromagnetic radiation that forms a characteristic conical wavefront. The opening angle θ_C of the emitted cone, measured with respect to the particle direction, is governed by the particle speed $v = \beta c$ and the refractive index η of the medium, according to:

$$\cos\theta_C = \frac{1}{\beta\eta} = \frac{\beta_{\rm thr}}{\beta}. \tag{1}$$

The spectral density of emitted photons is expressed by the Frank–Tamm relation:

$$\frac{d^2N}{dx\,d\lambda} = z^2\frac{2\pi\alpha}{\lambda^2}\sin^2\theta_C = z^2\frac{2\pi\alpha}{\lambda^2}\frac{\beta+\beta_{\rm thr}}{\beta^2}(\beta-\beta_{\rm thr}), \tag{2}$$

with z denoting the particle charge. Once the threshold velocity $\beta_{\rm thr}$ is exceeded, the photon production grows nearly linearly with β, and the emission spectrum is predominantly concentrated in the ultraviolet (UV) domain.

Because it provides a direct and non-destructive probe of particle velocity, Cherenkov radiation has become a standard technique in several branches of physics. In high-energy physics in particular, the measurement of both the cone angle and the number of produced photons enables effective particle identification. Its main drawback lies in the modest light yield: for instance, a relativistic singly-charged particle traversing water, plastic, or glass generates only ∼100–200 visible photons per centimeter of track. Moreover, a substantial fraction of the radiation occurs in the UV, where absorption in the medium and reduced detector sensitivity severely limit the detectable signal.

A well-known strategy to counter these limitations is the use of wavelength-shifting (WLS) additives in water or plastics, which absorb UV photons and re-emit them at longer wavelengths [1, 2]. Prominent examples are the application of 1,4-Bis(2-methylstyryl)benzene (bis-MSB) used in: WLS coatings [3], WLS plate collectors [4], or in acrylic Cherenkov modules such as those employed in the SuperTIGER experiment [5]. Nevertheless, the isotropic re-emission that characterizes the WLS effects makes the WLS doping unsuitable for Ring Imaging Cherenkov (RICH) devices, where the preservation of directional information is essential.

A further critical aspect for a Cherenkov radiator is the absence of parasitic scintillation. Certain commercial WLS plastics, including EJ-286, are known to produce residual scintillation signals [6, 7].

Within the framework of the PHeSCAMI project [8, 9], we have selected a material developed by *Glass to Power* [10] that acts as an efficient WLS for multi-stage UV conversion [7]. This compound, designated FB118, consists of polymethyl methacrylate (MMA) doped with 2,5-Bis(5-tert-butyl-benzoxazol-2-yl)thiophene (BBT). It shows excellent UV-to-visible conversion efficiency, which makes it an attractive option for high-performance Cherenkov radiators. A description of the preparation process and optical characterization of FB118 is given in [7].

In this work, we present a study of the response of FB118 to ionizing radiation. We report measurements carried out to quantify its Cherenkov photon yield and to verify the absence of scintillation background, and we assess its prospects for implementation in compact Cherenkov detectors for astroparticle physics.

2. Test of scintillation in FB118

We performed a comparative study of the light emission from an FB118 sample (9×4×1 cm^3) and an EJ-200 plastic scintillator with identical size. Two different experimental configurations were used: one for charged particle beams and cosmic muons, and another for γ-ray detection. In both cases, the samples were coupled to the same Hamamatsu R5946 photomultiplier tube (PMT) through optical grease. The charged-particle arrangement (Fig. 1A) consisted of two EJ-200

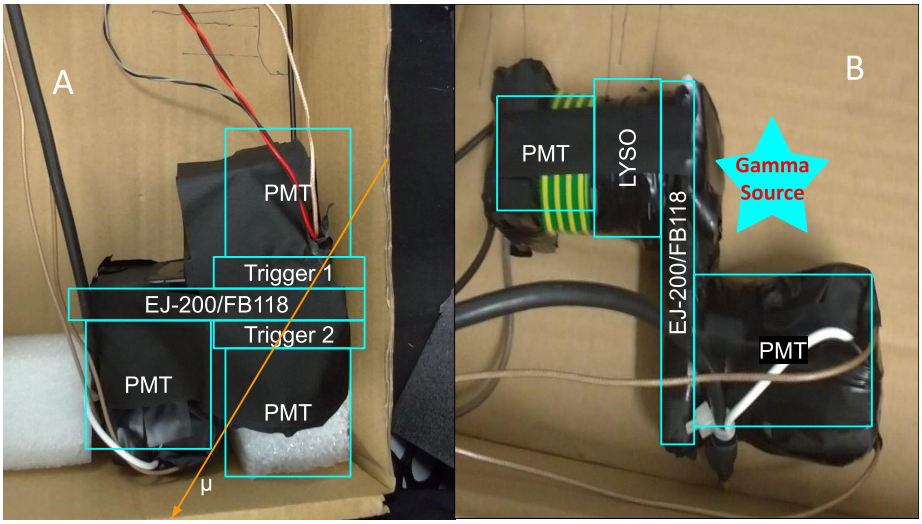

Figure 1: Pictures of the experimental layouts: (A) setup for charged particles; (B) setup for γ rays.

counters (Trigger1 and Trigger2) in telescope configuration, used to select atmospheric muons crossing either the FB118 or the EJ-200 test sample. The same system was also transported to the Trento Proton Therapy Center, where it was exposed to protons in the range 74–225 MeV. Since the acquisition relied on an external trigger, no amplitude thresholds were imposed on the signals recorded from the FB118 or EJ-200 blocks. As expected, Fig. 2 (top) shows that EJ-200 yields distributions consistent with the Bethe–Bloch prediction: lower proton energies correspond to larger energy depositions.

In contrast, the FB118 spectra (bottom) display negligible responses to protons, pointing to the absence of any appreciable scintillation. This behavior demonstrates that the emission in FB118 is essentially of Cherenkov origin. The Cherenkov threshold for protons in FB118, given its refractive index $\eta \simeq 1.5$, is approximately 320 MeV. Table 1 summarizes the most probable values (MPVs) of the measured amplitude distributions for the different particle types and energies.

Table 1: Most probable values (MPVs) of the signal amplitudes measured with p and μ in EJ-200 and FB118.

Particle	p 74 MeV	p 83 MeV	p 100 MeV	p 225 MeV	μ
MPV EJ-200	9.04 ± 0.08	8.25 ± 0.04	7.42 ± 0.05	3.55 ± 0.06	2.0 ± 0.1
MPV FB118	0.001 ± 0.003	0.014 ± 0.001	0.024 ± 0.001	0.018 ± 0.003	0.22 ± 0.01

For muons, the ratio of light yield between EJ-200 and FB118 is $9.1 \pm 0.6^{(\text{stat.})} \pm 2.5^{(\text{syst.})}$, where the systematic component reflects differences in PMTs, operating voltages, and optical contacts.

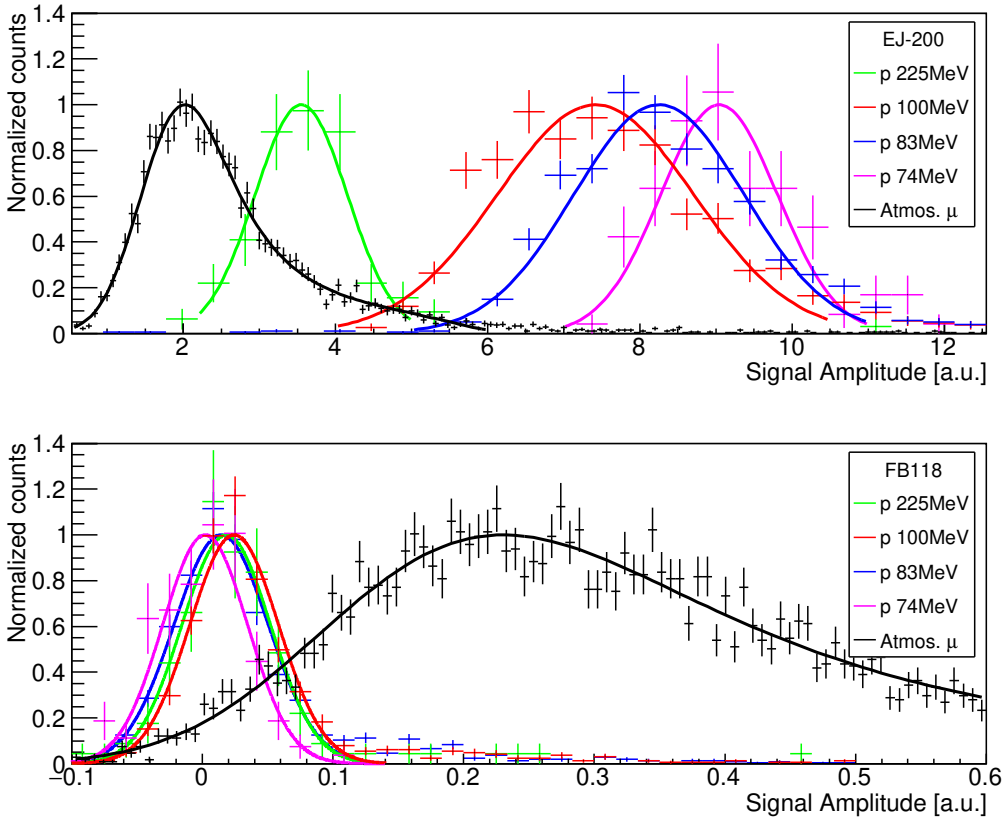

Figure 2: Signal amplitude spectra for protons and μ: EJ-200 (top) and FB118 (bottom).

The second setup (Fig. 1B) addressed the γ-ray response, using an 8 g LYSO crystal as a source of internal ^{176}Lu activity (emitting mainly 202, 307, and 401 keV photons). Coincidences between LYSO and the test samples were employed as triggers. Further measurements were performed with a ^{60}Co source, producing 1173 and 1332 keV γ rays. Because both plastics have low effective atomic numbers, only Compton scattering contributes to the signals, resulting in continuous distributions. The LYSO source mainly generates sub-threshold electrons (the Cherenkov threshold for electrons in FB118 is ~170 keV), while the higher-energy photons from ^{60}Co produce a significant fraction of above-threshold electrons. As displayed in Fig. 3, FB118 exhibits a stronger response to the ^{60}Co source, consistent with the expectation of Cherenkov-dominated emission.

From the ^{60}Co runs, the residual scintillation in FB118 is constrained to be less than 10% of that of EJ-200. The LYSO data suggest an even stronger suppression, up to a factor of 30, whereas the proton-beam results limit the fraction to below 0.3%. Taking into account the known EJ-200 light yield (~10,000 photons/MeV), the muon data imply that FB118 produces about 200 visible photons per millimeter, originating from Cherenkov emission. This relatively high yield can be attributed to the ability of FB118 to efficiently absorb UV photons and re-emit them in the visible.

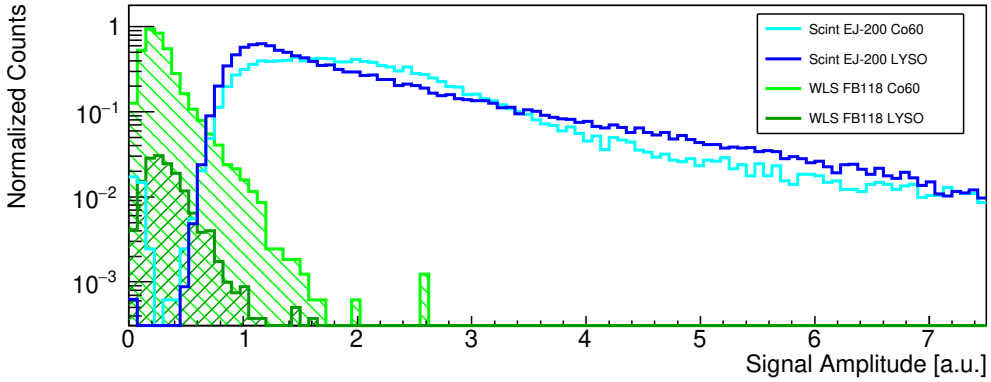

Figure 3: Distributions of γ-ray signal amplitudes. FB118 (shaded histogram) shows a much lower response than EJ-200 (open histogram).

3. Velocity reconstruction with FB118 Cherenkov signals

We investigated the possibility of exploiting FB118 to measure particle velocity through its Cherenkov emission. To this end, a Time-of-Flight (ToF) apparatus was constructed using six EJ-200 scintillator slabs (30×25×1 cm^3): three modules placed on the floor and three directly above them on the ceiling, with a vertical separation of 5.1 m (Fig. 4). The readout relied on a CAEN DT5742 digitizer (5 GS/s), enabling the determination of inverse velocity $1/\beta_{\mathrm{ToF}}$ with a precision of about 8%. This accuracy was mainly limited by fluctuations in the propagation time of scintillation light within the EJ-200 tiles, which depend on the random particle crossing point.

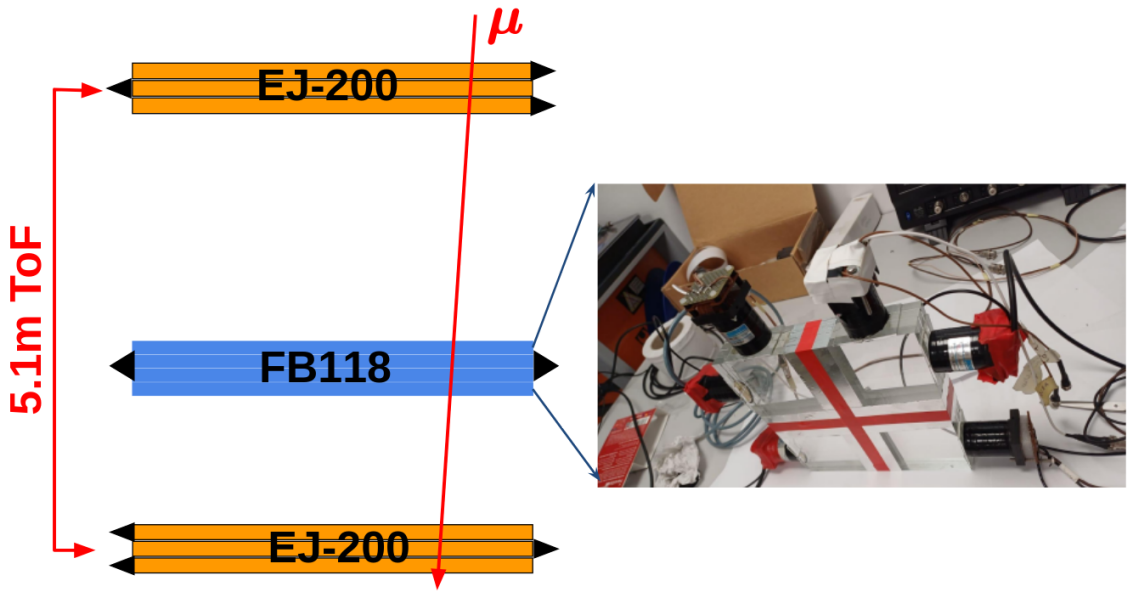

Figure 4: Layout of the ToF system used to compare the velocity derived from FB118 Cherenkov light with that obtained from the timing difference between top and bottom EJ-200 scintillator layers.

At the center of the ToF telescope, a dedicated Cherenkov detector based on FB118 was

installed (inset of Fig. 4). It consisted of four stacked FB118 plates (24×24×1 cm^3), each optically coupled to a set of six Hamamatsu R5946 PMTs. During operation indoors, the system collected 11.3k triggers, predominantly induced by relativistic atmospheric muons. The $1/\beta_{\mathrm{ToF}}$ distribution revealed that roughly 2% of the events correspond to slower particles.

Figure 5(a) reports the average signal amplitude recorded in the EJ-200 scintillators as a function of $1/\beta_{\mathrm{ToF}}$. The solid black curve illustrates the expected dependence according to the Bethe–Bloch energy-loss law. Panel (b) of the same figure shows the mean amplitude of the FB118 Cherenkov signals, compared with the prediction from the Frank–Tamm equation (Eq. 2). As anticipated, no light is observed below the Cherenkov threshold, located at $1/\beta_{\mathrm{thr}} = \eta$ (vertical dashed line).

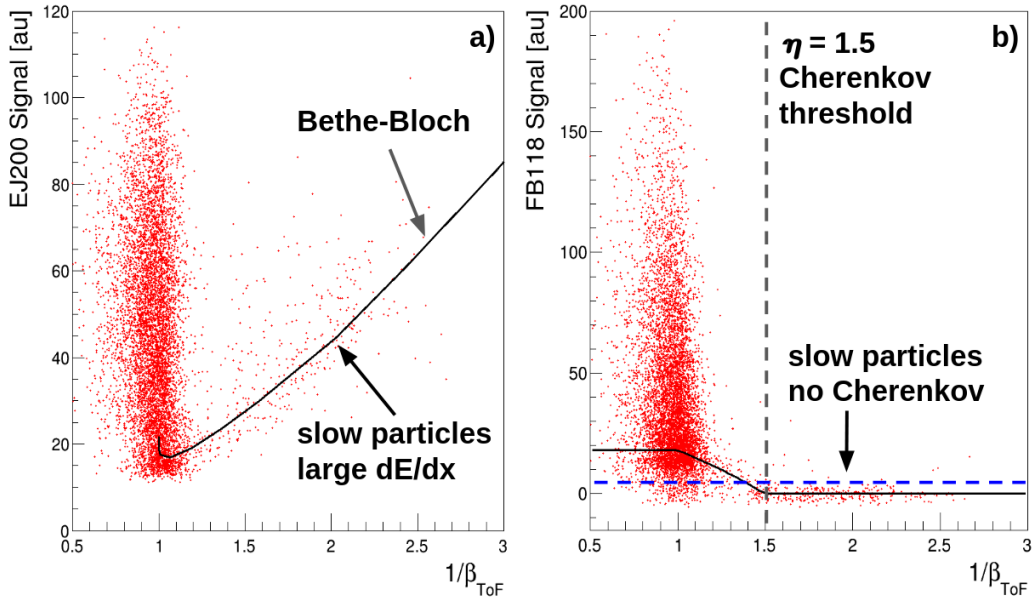

Figure 5: (a) Average scintillation amplitude from EJ-200 versus inverse velocity measured with ToF. The curve corresponds to Bethe–Bloch expectations. (b) Average Cherenkov amplitude from FB118 compared with the Frank–Tamm prediction. The dashed vertical line indicates the Cherenkov threshold.

These results highlight the role of FB118 as an efficient Cherenkov radiator for compact astroparticle detectors. In fact, ToF systems are usually impractical in such experiments because of strict limitations in size and power consumption. Scintillation signals alone make it difficult to discriminate slow particles from the Landau tails of the large relativistic flux, see Fig. 5(a). Conversely, the horizontal dashed blue line in Fig. 5(b) demonstrates that a Cherenkov-based cut is very effective in tagging sub-relativistic particles.

This is further illustrated in Fig. 6 (left), where events with FB118 signals below 0.25 of the saturation level are shown to correspond almost exclusively to slow particles, with only about 1.5% contamination from minimum-ionizing (MIP) events. Such a selection corresponds to $\beta < 0.7$, which for protons implies kinetic energies below 400 MeV. This functionality would be highly valuable in compact instruments such as NUSES/Zirè [11], where it could provide straightforward electron–hadron discrimination.

Large-scale future missions aiming at the detection of stopped antinuclei in cosmic rays [12] will face high trigger rates from relativistic protons and electrons. Employing FB118 as a Cherenkov

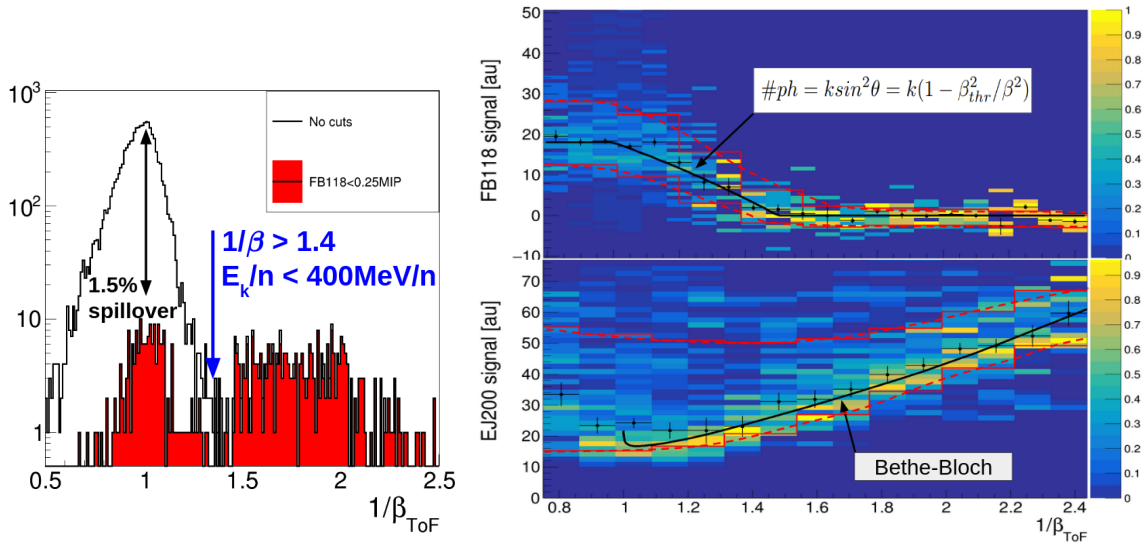

Figure 6: Performance of velocity determination with FB118. Left: selection of FB118 signals below 0.25 of the saturation (MIP) level identifies mainly slow particles (red-filled histogram). Right, top: FB118 signal amplitude versus β, consistent with Frank-Tamm expectation. Right, bottom: EJ-200 signal amplitude versus β, consistent with Bethe–Bloch behavior. By combining the two, particle velocity can be reconstructed with ~20% resolution without a ToF system.

veto at the trigger stage could reduce these rates by roughly an order of magnitude.

Finally, velocity information can be extracted from the Bethe–Bloch law in the non-relativistic regime ($\beta < 0.7$) using scintillator or silicon detectors. This is visible in Fig. 6 (bottom-right), where the normalized EJ-200 signal follows the Bethe–Bloch curve. In the relativistic region ($\beta > 0.7$), the FB118 Cherenkov amplitude provides complementary sensitivity, see Fig. 6, top-right. Taken together, the two observables yield a velocity resolution better than 20%, opening the possibility to replace an entire ToF system in space-borne compact detectors.

4. Conclusions

We carried out a detailed characterization of the optical response of FB118, the wavelength-shifting plastic produced by "Glass to Power" [10]. No significant residual scintillation was detected (below 30 ph./MeV), thus satisfying one of the essential conditions for its implementation within the PHeSCAMI detector [8, 9, 12].

On the other hand, FB118 exhibited an intense Cherenkov signal (~200 ph./mm), amplified by the excellent UV-to-visible conversion efficiency of the material. This makes FB118 particularly attractive as a compact Cherenkov radiator in the velocity interval $0.7 \lesssim \beta \lesssim 0.9$, with specific relevance for lightweight, space-borne instruments where conventional Time-of-Flight systems are not feasible.

In parallel, we are initiating the development of aerogel (AGL) radiators ($\eta_{AGL} \sim 1.05$) doped with WLS fluors at the INFN/TIFPA laboratories. Due to the relatively high Cherenkov threshold of aerogel ($E_K > 2$ GeV for protons), such radiators are expected to play a key role in reducing trigger rates in upcoming large-scale spectrometers, such as ALADInO [13].

Acknowledgments

We thank A. Pavlovic for providing the FB118 sample. This work was supported by the Italian PRIN-2022 grant n. 2022LLCPMH "PHeSCAMI – Pressurized Helium Scintillating Calorimeter for AntiMatter Identification," CUP E53D23002100006.

References

[1] G. Badino, et al., *The effect of wavelength shifters on water Cherenkov detectors*, Nuclear Instruments and Methods in Physics Research **185** (1981) 587–589.

[2] E. P. Krider, et al., *Wavelength-shifted Cherenkov radiators*, Nuclear Instruments and Methods **134** (1976) 495–503.

[3] M. Grande, G. R. Moss, *An optimised thin film wavelength shifting coating for Cherenkov detection*, Nuclear Instruments and Methods in Physics Research **215** (1983) 539–548.

[4] R. Claus, et al., *A waveshifter light collector for a water Cherenkov detector*, NIM A **261** (1987) 540–542.

[5] R. P. Murphy, et al., *In-flight Performance of the Super-TIGER Cherenkov Counters*, Proc. 33rd International Cosmic Rays Conference (ICRC 2013), Sociedade Brasileira de Fisica (2013).

[6] Eljen Technology, *Wavelength Shifting Plastics: EJ-280, EJ-282, EJ-284, EJ-286* (2024). Available at: https://eljentechnology.com/products/wavelength-shifting-plastics/ej-280-ej-282-ej-284-ej-286 [Accessed: 19 July 2025].

[7] C. Brizzolari, et al., *Enhancement of the X-Arapuca photon detection device for the DUNE experiment*, Journal of Instrumentation **16** (09) (2021) P09027. doi:10.1088/1748-0221/16/09/P09027.

[8] F. Nozzoli, et al., *Antideuteron Identification in Space with Helium Calorimeter*, Instruments **8** (1) (2024) 3. doi:10.3390/instruments8010003.

[9] L. E. Ghezzer, et al., *Development of a Pressurized Helium Scintillating Calorimeter for AntiMatter Identification*, PoS **EXA-LEAP2024** (2025) 048. doi:10.22323/1.480.0048.

[10] Glass to Power SpA, *Wavelength Shifters – Nanotechnologies* (2024). Available at: https://www.glasstopower.com/wavelength-shifters/ [Accessed: 19 July 2025].

[11] NUSES Collaboration, *The Ziré instrument onboard the NUSES space mission*, Nucl. Instrum. Meth. A **1068** (2024) 169794. doi:10.1016/j.nima.2024.169794.

[12] L. E. Gezzer, F. Nozzoli *et al.*, *Advancing Anti-Deuteron Detection in Cosmic Rays: Innovations in Methods and Technologies*, PoS **ICRC2025** (2025) 508.

[13] O. Adriani *et al.* [ALADInO Collaboration], *Design of an Antimatter Large Acceptance Detector In Orbit (ALADInO)*, Instruments **6** (2) (2022) 19. doi:10.3390/instruments6020019.